Journal of Metals, Materials and Minerals, 33(4), 1785, 2023

Effect of calcination frequency on the thermoelectric properties of Ti doped $CuCrO_2$ by solid state method

Doli BONARDO[1,*], Nono DARSONO[2], Syahrul HUMAIDI[3], Agung IMADUDDIN[2], and Noni Surtiana SILALAHI[3]

[1] *Refrigeration and Air Conditioning Engineering Study Program, Politeknik Tanjungbalai, Jl. Sei Raja, Sei Tualang Raso, Tanjungbalai, 21345, Indonesia*
[2] *Research Center for Advanced Materials, National Research and Innovation Agency (BRIN), Tangerang Selatan, Banten, 15314, Indonesia*
[3] *Post Graduate Program (Physics), FMIPA, Universitas Sumatera Utara, Jl. Bioteknologi I Kampus USU, Medan, 20155, Indonesia*

***Corresponding author e-mail:** hasanbonardo@gmail.com

Received date:
6 July 2023
Revised date
8 November 2023
Accepted date:
9 November 2023

Keywords:
Thermoelectric material;
$CuCrO_2$;
TiO_2;
Delafossite;
Solid-state

Abstract

In this study, the influence of titanium oxide (TiO_2) dopants and varying calcination processes on the thermoelectric properties of $CuCrO_2$ was systematically explored. It was emphasized that these factors were not only affecting dislocation density but also exerting a profound influence on thermoelectric performance through the modulation of Seebeck coefficient and resistivity. The findings highlighted CrT-2, which incorporated TiO_2 and underwent a two-time calcination process, as the top-performing sample in terms of power factor values, underscoring the significance of TiO_2 as a dopant for enhancing thermoelectric efficiency. Conversely, Cr-4, exposed to four calcination cycles, exhibited slightly lower power factor values compared to Cr-2. Notably, CrT-4, despite containing the titanium dopant, showed the lowest power factor values, potentially due to intricate interactions between the dopant and the extended calcination process. These results underscore the intricate interplay between dopants, calcination processes, and thermoelectric performance in $CuCrO_2$, necessitating precise optimization to achieve the desired material efficiency.

1. Introduction

In the last decades, the delafossite structure has become a subject of study that has attracted a lot of attention to scientists because of its unique combination of electrical conductivity and high transparency for visible light. In addition, it has good thermoelectric, optoelectric, electrical and magnetic properties [1]. So that in the development of new material applications it becomes an important part of technological and industrial progress in all fields [2,3].

Researchers have carried out various innovations in developing the synthesis of various insulator and conductor materials which are varied with various doping so that innovations emerge in creating new materials such as delafossite $CuCrO_2$, $CuAlO_2$, $CuFeO_2$, and so on [4]. Among the many studies conducted, $CuCrO_2$ research is being intensively carried out because it is reported to have high conductivity properties [5], so that it becomes a new breakthrough in the development of modern and efficient materials and semiconductors [6]. In addition, the potential that delafossite has in its application is very broad, including in industry and technology as TCO (Transparent Conducting Oxides) [7]. This TCO is applied to sensors and diodes. Several other high-tech equipments such as plate panels, touch screens, and thin film batteries use the TCO principle [8].

$CuCrO_2$ is one of the most interesting delafossites because it is a compound that is easily oxidized, and it is hoped that the $CuCrO_2$ compound will have a high conductivity [9] However, its electrical properties, especially when it was affected by temperature, is a challenge for researchers. This thermoelectric property is exclusively owned by $CuCrO_2$ because of its electronic structure which allows electrons to move freely when influenced by the temperature of the material. However, the development of this property still has wide opportunities because various modifications can continue to be made such as adding additives to increase the synergistic effect, preparation methods that can determine the nature of the crystals, or even adding catalysts to improve the quality and quantity of thermoelectricity property [10]. One that becomes important in improving the thermoelectric properties of materials is their conductivity. This property is the foundation for how thermoelectrical works according to the capabilities of the material, because conductivity reflects the ability of a material to accommodate the transfer of electrons in its electronic structure [11].

To improve the conductivity properties of $CuCrO_2$ as a thermoelectric material with TCOs technology, using dopants is one strategy that can be done because additives can help modify the overall electronic structure of the material [12]. In addition, its presence is expected to support the improvement of physical and mechanical properties. Currently, on the scale of the electronics industry, various types of impurity materials are used as doping for $CuCrO_2$ [13]. The four major dopings are Ti, Mg [14], Ni and Co. Among them, the metal ions of Ti are most strongly incorporated at the Cr site so that they can enhance the electrical properties by increasing the number of electrons captured in the electronic structure of the material [15]. The indicator of an

increase in the electrical properties of the $CuCrO_2$ delafossite is a decrease in the resistivity value of the material so that the conductivity increases, the Seebeck coefficient also needs to be observed to find out how far the thermoelectric sensitivity of the material changes in terms of temperature functions, the increase in power factor due to certain modifications is one of the final considerations to determine the electrical properties of the thermoelectric materials [13,16,17].

Various methods of synthesis of $CuCrO_2$ have been carried out, such as sol-gel techniques, solid state reaction, hydrothermal synthesis, chemical vapor deposition, pulsed laser deposition, electron beam evaporation, sputtering, and so on [13]. However, the solid state reaction method is more interesting because it offers a very short reaction time, an efficient reaction and the collection process of reaction products is also very easy among other methods [18]. In this technique, several factors that can affect the reaction that takes place are the chemical and morphological properties of reagents including the reactivity, surface area, and free energy change with the solid state reaction, and other reaction conditions, such as the temperature, pressure, and the environment of the reactions [19]. One of the things that is interesting to understand is how the reaction temperature can affect the resulting product, where the key temperature referred to here is the calcination temperature [9]. Calcination can be defined as the process in which the ore of the metal is heated to high temperature in the absence or limited supply of air or oxygen [20]. In solid state reactions, the main objective of the calcination process is to remove impurities so as to increase the purity of the desired product phase [21]. So in this work, Ti-doped $CuCrO_2$ was synthesized by a solid state reaction process with TiO_2 as the source of Ti. In addition, calcination treatment in solid state reactions (two times and four times) was carried out. The addition of Ti dopant and the calcination route is expected to improve the performance of the thermoelectric properties of $CuCrO_2$.

The novelty of this research lies in the strategic use of dopants, specifically titanium (Ti), to modify the electronic structure of $CuCrO_2$. This innovative approach not only seeks to improve the material's electrical conductivity but also aims to enhance its physical and mechanical properties. Furthermore, the study explores various calcination routes (two times and four times) during the solid-state reaction process, offering a unique perspective on how the calcination temperature affects the resulting product. This research opens up new avenues for tailoring the thermoelectric performance of $CuCrO_2$, paving the way for advancements in the development of efficient and modern materials with applications in diverse fields, from electronics to sustainable energy technologies.

2. Experimental

2.1 Materials and procedures

CuO, TiO_2, and Cr_2O_3 precursors were purchased from Sigma-Aldrich Co. and used in the synthesis. A stoichiometric amount of 0.05 wt% TiO_2 (0.025 g) was mixed with 0.51 g Cr_2O_3 and 0.463 g CuO. The mixture was then ground using a mortar for 3 h to achieve a smooth sample consistency. For the double calcination process, the sample was subjected to firing at 1000°C for 10 h, followed by gradual cooling to room temperature (25°C) inside the furnace. Subsequently, the precursor was re-ground for an additional 3 h to further refine the clumped grains. In the next stage, the ground precursor was fired again at 1050°C for 10 h, and once again cooled to room temperature in the furnace. Re-grinding was carried out for an additional 3 h. The resulting pure $CuCrO_2$ was pelletized and subjected to annealing at 1100°C to increase the sample density. For the four calcination processes, the samples underwent firing at 1000°C, then 1050°C, followed by 1100°C, and finally 1150°C, before pelletization and subsequent annealing at 1100°C. After each firing process, the sample was allowed to cool inside the furnace until it reached room temperature, followed by crushing to refine the material consistency, mirroring the procedure employed for the double calcination method described earlier. As a control, samples without the addition of Ti were synthesized and treated in the same manner as those with the Ti dopant. The design and composition of each sample are presented in Table 1.

2.2 Material characterization

After all samples were successfully synthesized, they were characterized using a scanning electron microscope (Hitachi S-4800) to determine the surface morphology of the sample, X-Ray Diffraction (Bruker D8 Advance) to determine phase formation, and then resistivity testing and Seebeck coefficient to determine the electrical properties were obtained with Keithley 237, 236 source-measure units and HP 3458A and Agilent 3458A multimeters. To generate a temperature differential (ΔT), a specially designed temperature control system was employed. This system included a precision temperature controller and heating elements, enabling precise temperature control within the desired range of 100°C to 500°C.

In accordance with best practices for thermoelectric measurements, the system was calibrated using a standard reference material. The choice of the reference material, as well as the calibration procedure, were meticulously carried out to ensure the accuracy and reliability of the measurements. The calibration process involved known thermoelectric standards to verify the system's performance.

Table 1. Design and compositions of samples.

Samples label	Ti (wt%)	Calcination process
Cr-2	0	Two times
Cr-4	0	Four times
CrT-2	0.05	Two times
CrT-4	0.05	Four times

3. Results and discussion

Figure 1 showcases SEM images of the Cr-2 sample at magnifications of 5000x and 10000x. At 5000x magnification, it's evident that the surface features a uniform distribution of grains with high density, and grain orientations show some overlap. The typical delafossite morphology of agglomerated crystal grains with different sizes is observed. At 10000x magnification, the grain structure is less uniform and dispersed, with relatively large and uneven grain sizes, leading to the formation of larger pores. Grain boundaries are distinct, contributing to the open sides of the grains [8]

Figure 2 illustrates the Cr-4 sample, which underwent double the calcination cycles of Cr-2. This sample exhibits a more even grain distribution, with reduced empty space on the surface. The surface structure is denser than Cr-2, and grain orientations tend to be consistent. At 10000x magnification, grain gaps are narrower, and grain volumes tend to increase, indicating increased agglomeration in the surface structure. Compared to the Cr-2 sample, the surface of the Cr-4 sample appears flatter and smoother, suggesting that the grain orientation structure has been compromised [22], resulting in a rougher surface for the Cr-2 sample.

In contrast, the CrT-2 sample, with 0.05 wt% titanium oxide, demonstrates noteworthy differences. The microstructure is characterized by optimal grain orientation, even distribution, and homogeneous dispersion, resulting in reduced porosity compared to the undoped samples (see Figure 3). The grain size also increases due to the presence of Ti particles, which promote higher activation energy. The surface of the CrT-2 sample exhibits a noticeably smoother texture compared to the grains on the surface of the CrT-4 sample. A striking distinction between the CrT-2 and CrT-4 samples is the presence of Titanium (Ti) particles on the surface of the sample grains, which is absent in both the Cr-2 and Cr-4 samples.

Figure 4 displays the CrT-4 sample, which experienced both titanium oxide addition and four calcination cycles. While the grain distribution is lower than CrT-2, the addition of Ti dopants led to grain fragmentation, as larger spherical grains became smaller grains. The grains in CrT-4 appeared smaller and denser, marking a significant contrast with the other three samples. The quantitative analysis of the grain size and size distribution across the four samples reveals a consistent trend. In all cases, including the Cr-2, Cr-4, CrT-2 (with 0.05 wt% TiO_2), and CrT-4 (with 0.05 wt% TiO_2), grain sizes predominantly fall within the range of 1 µm to 4 µm. However, there are fluctuations in the size distribution, likely stemming from variations in SEM image analysis.

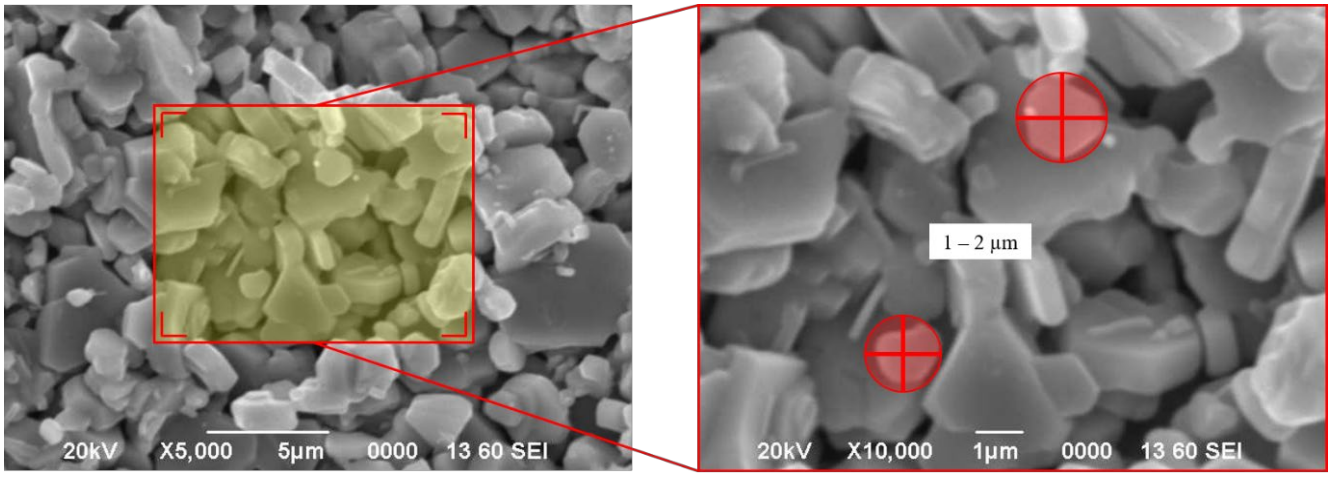

Figure 1. SEM image of Cr-2 with 5000 times and 10000 times magnification.

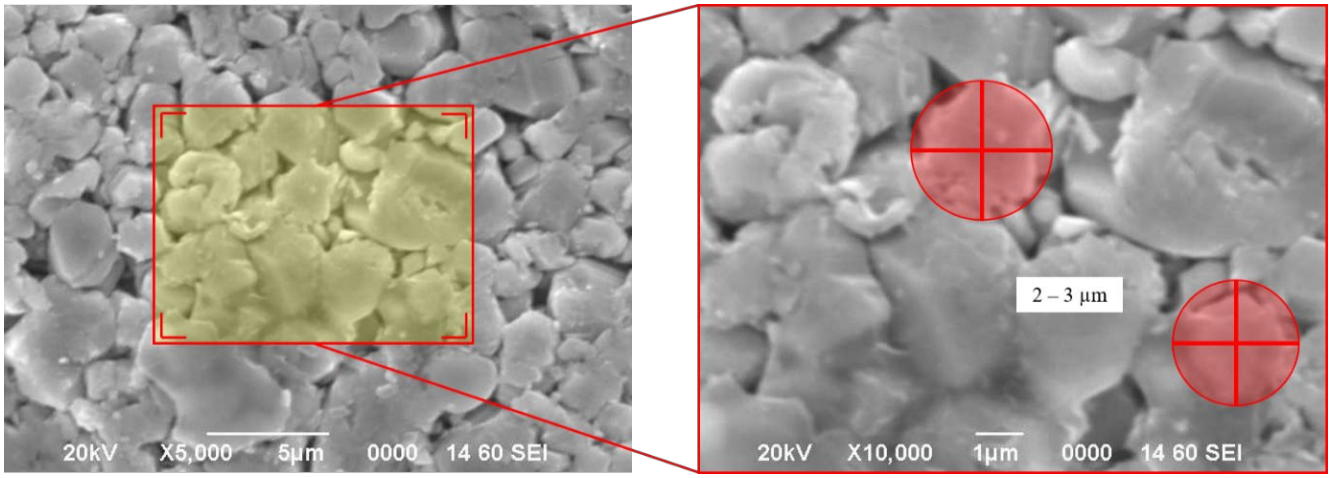

Figure 2. SEM image of Cr-4 with 5000 times and 10000 times magnification.

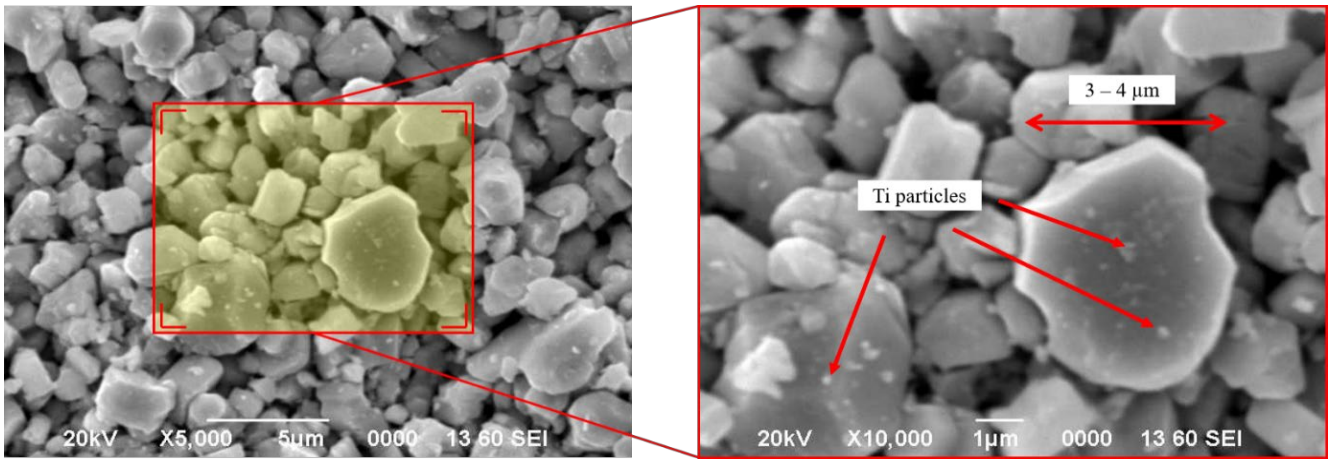

Figure 3. SEM image of CrT-2 with 5000 times and 10000 times magnification.

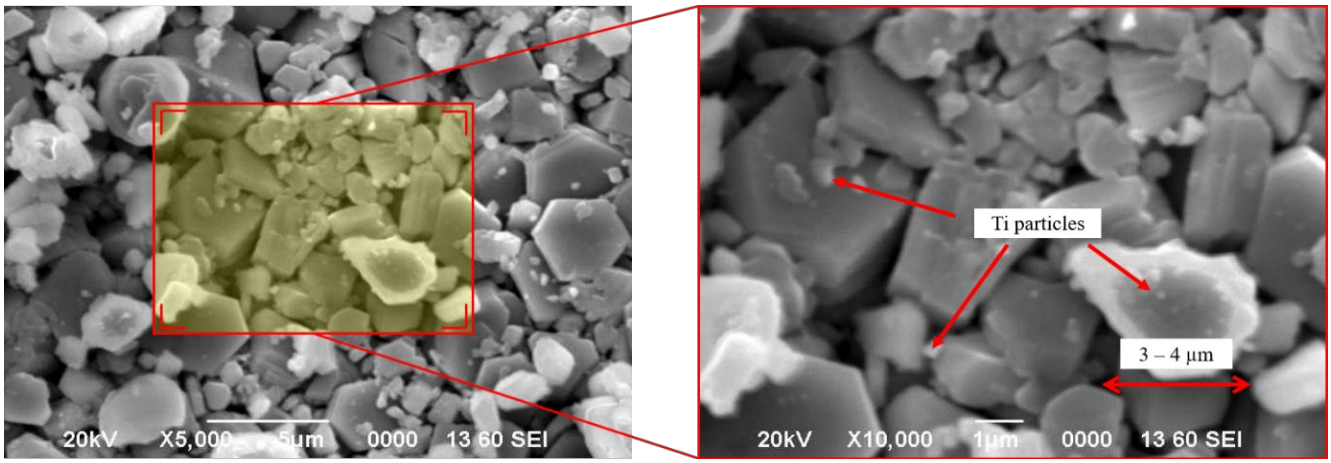

Figure 4. SEM image of CrT-4 with 5000 times and 10000 times magnification.

Figure 5 shows the XRD diffraction patterns on Cr-2, Cr-4, CrT-2, and CrT-4 samples in the 2θ 5° to 85° range. In general, the four samples exhibit identical diffraction patterns to one another. All samples also showed crystal peaks associated with the $CuCrO_2$ crystal phase without any detectable impurities, in other words the phase that appeared had a relatively high degree of purity. However, the presence of the Ti dopant had an effect on the diffraction pattern formed, where after the addition of Ti, the phases formed were $CuCrO_2$, and TiO_2 with high crystalline intensity. Of these phases the most dominant is the $CuCrO_2$ phase [10]. They present a broad and slight pick diffraction of 25°, 37.3°, 52.1° and 55.7° 2θ related to the hydrotalcite. The resulting reflection confirmed that the sample carried out was a single-phase type-p $CuCrO_2$ delafossite material. The addition of Ti in $CuCrO_2$ has an effect in producing phase peak changes in the sample, at some peaks the addition of Ti can reduce the peak intensity of the $CuCrO_2$ phase, but the addition of Ti does not change the structure or lattice parameters formed in the sample, so that the synthesis of $CuCrO_2$ delafossite has been successfully carried out [9].

Table 2 shows the average crystallite size and dislocation density of the samples based on the FWHM value and 2θ resulted. Analyzing the data from Table 2, it's apparent that the addition of titanium dopant (CrT-2 and CrT-4) does not significantly impact the crystallite size when compared to the undoped samples (Cr-2 and Cr-4). The variations in crystallite size among the samples are relatively minor, suggesting that the presence of titanium oxide has a limited effect on crystallite growth. Furthermore, the number of calcination cycles (two times or four times) does not result in substantial differences in crystallite size, as the variations between Cr-2 and Cr-4, and CrT-2 and CrT-4 remain relatively slight.

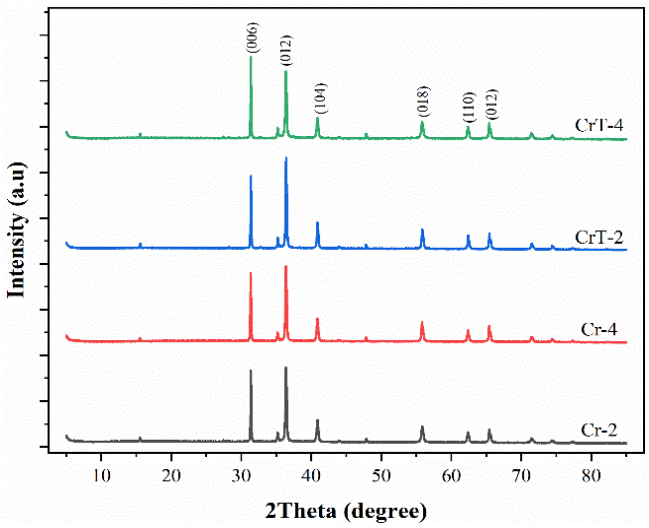

Figure 5. XRD pattern of $CuCrO_2$ with different amount of Ti dopants.

Table 2. Crystallite size and dislocation density of the samples.

Samples	Average FWHM (rad)	Average crystallite size (nm)	Average dislocation density (x10^{-4} nm^{-2})
Cr-2	0	Two times	
Cr-2	0.279	35.51	9.569
Cr-4	0.270	36.14	8.424
CrT-2	0.257	38.17	8.013

An intriguing observation is the connection between dislocation density and the Seebeck coefficient values. Generally, samples with higher dislocation densities (Cr-2 and CrT-4) exhibit elevated Seebeck coefficients. This relationship suggests that increased grain boundaries and defects, often associated with higher dislocation densities, can contribute to enhanced thermoelectric properties [22]. However, it's important to note that higher dislocation densities can also limit carrier mobility within the $CuCrO_2$ system, potentially leading to a reduction in the power factor [20,23].

$CuCrO_2$ is a p-type semiconductor, where its resistivity decreases with increasing temperature [7,24]. This is because of increasing temperature, the electrons in the valence band gain sufficient thermal energies to jump to the conduction band. As the number of electrons in the conduction band increases, so conductivity increases and resistivity decreases [25]. The resistivity-temperature relationship, as shown in Figure 6, provides valuable insights into the electrical behavior of the four different samples (Cr-2, Cr-4, CrT-2, and CrT-4) in the temperature range of 100°C to 500°C. The graph clearly demonstrates the distinct variations in resistivity for each sample composition. Notably, the sample CrT-2 exhibits the lowest resistivity throughout the entire temperature range [18]. This reduction in resistivity can be attributed to the presence of the titanium dopant, which enhances the electrical conductivity of the material. The calcination process (2 times) appears to have a favorable effect on the electrical behavior, likely by reducing impurities or defects in the material structure [12].

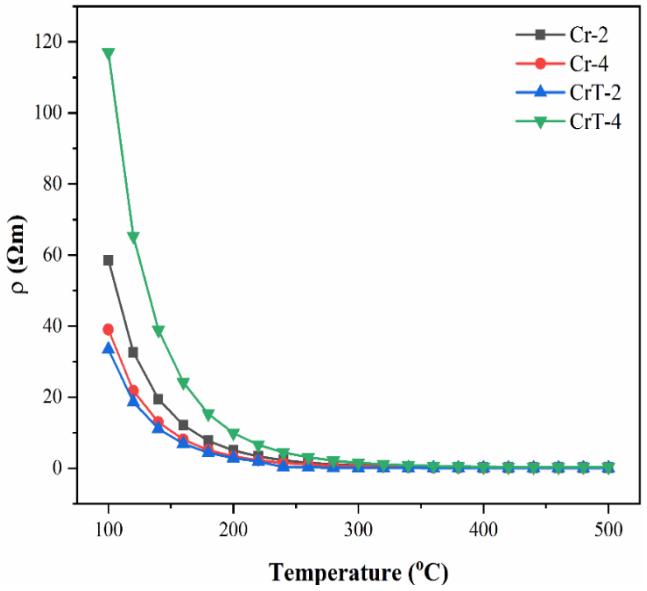

Figure 6. Electrical resistivity of different $CuCrO_2$ samples as a function of temperature.

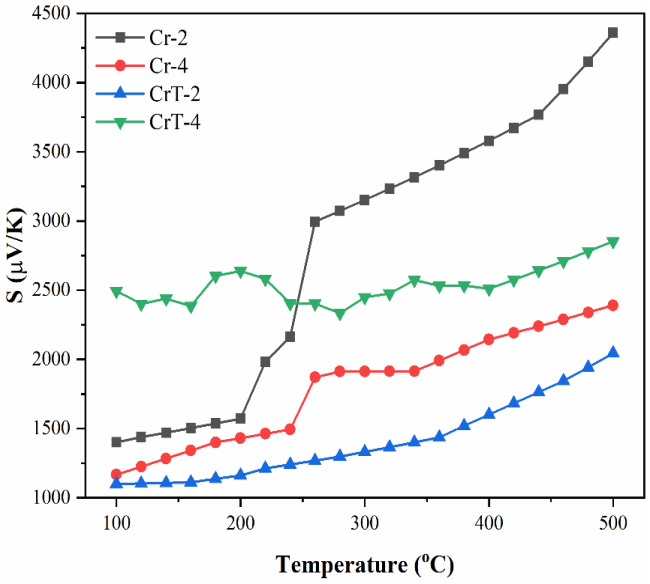

Figure 7. Seebeck coefficient of different $CuCrO_2$ samples as a function of temperature.

Cr-4 follows CrT-2 in terms of resistivity, demonstrating slightly higher resistivity values. The four-time calcination process contributes to a reduction in resistivity compared to Cr-2. While Cr-4 lacks the titanium dopant, the additional calcination cycles enhance the material's electrical properties. The undoped sample Cr-2 exhibits resistivity values higher than CrT-2 and Cr-4. The two-time calcination process contributes to improved electrical conductivity compared to the non-calcined state. However, CrT-4 demonstrates the highest resistivity among the four samples, despite the titanium dopant. The combination of a longer calcination process (4 times) and the titanium dopant may contribute to this effect. The longer calcination cycles might introduce defects or impurities that counteract the dopant's positive influence, leading to higher resistivity [15].

The order of resistivity values, from lowest to highest, is CrT-2, Cr-4, Cr-2, and CrT-4 suggests that the addition of 0.05 wt% titanium oxide (TiO_2) is effective in reducing resistivity, as observed in CrT-2. Furthermore, the number of calcination cycles plays a significant role in modifying the electrical properties. Longer calcination times, as seen in Cr-4 and CrT-4, generally lead to decreased resistivity, potentially by eliminating impurities or enhancing material crystallinity [6,9,16]. These findings emphasize the intricate relationship between sample composition, calcination processes, and electrical properties, shedding light on the potential for optimizing thermoelectric materials for various applications.

Figure 7 shows the Seebeck coefficient as a function of temperature for four $CuCrO_2$ samples. CrT-4 sample has the highest Seebeck

coefficients of ~1921 $\mu V \cdot K^{-1}$ at 300 K. The Seebeck coefficients of the CrT-2 exhibits the lowest Seebeck coefficient values across the entire temperature range. The presence of titanium dopant contributes to a reduced Seebeck coefficient. The two-time calcination process further minimizes the Seebeck coefficient, suggesting that this combination of factors results in less efficient thermoelectric performance [26,27]. Cr-4 follows CrT-2 in terms of the Seebeck coefficient. It demonstrates slightly higher Seebeck coefficient values, which can be associated with the four-time calcination process. These additional calcination cycles enhance the thermoelectric properties to some extent.

The undoped sample Cr-2 exhibits Seebeck coefficient values higher than CrT-2 but lower than Cr-4. The two-time calcination process contributes to improved thermoelectric performance compared to the non-calcined state. Notably, CrT-4 exhibits the highest Seebeck coefficient values among the four samples. However, its behavior is marked by fluctuations in the range of 100°C to 170°C. These fluctuations indicate an unstable thermoelectric response within this temperature range. The Seebeck coefficient values increase as the temperature rises to 200°C, suggesting improved thermoelectric behavior. They then decrease as the temperature rises to 280°C, indicating a temporary decline in performance. The values rise again when the temperature reaches 340°C, drop only slightly at 400°C, and rise once more at 500°C. The presence of titanium oxide (TiO_2) generally leads to lower Seebeck coefficient values, and The fluctuations in the Seebeck coefficient of CrT-4 may result from complex interactions between dislocation density, temperature, and the presence of the titanium dopant [11,28].

Basically the decrease in electrical resistivity upon doping leads to an increased power factor (PF) $S^2.\sigma$, where S is the Seebeck coefficient and σ is the electrical conductivity [4]. The graph in Figure 8 illustrates the power factor-temperature relationship for four different samples (Cr-2, Cr-4, CrT-2, and CrT-4) over a temperature range of 100°C to 500°C. The power factor, which is a key indicator of thermoelectric efficiency, reveals distinct trends among the samples. Notably, CrT-2 exhibits the highest power factor values across the entire temperature range. The presence of the titanium dopant in this sample significantly enhances its thermoelectric performance. Additionally, the two-time calcination process seems to have a positive impact on improving the power factor, making CrT-2 the most efficient thermoelectric material among the studied samples.

Cr-2 (Calcination 2 times) closely follows CrT-2 in terms of power factor, displaying slightly lower values but still outperforming the other two samples. The two-time calcination process contributes to improved thermoelectric properties in Cr-2. On the other hand, Cr-4 (Calcination 4 times) exhibits a slightly lower power factor than Cr-2. The four-time calcination process enhances its thermoelectric efficiency but falls short of the performance observed in Cr-2 and CrT-2. Despite the presence of the titanium dopant, CrT-4 (0.05 wt% TiO_2, Calcination 4 times) displays the lowest power factor among the samples. This suggests that the combination of the titanium dopant and the longer calcination process might introduce complex interactions that negatively impact thermoelectric efficiency.

CrT-2 stands out as the most efficient thermoelectric material, demonstrating the potential of titanium oxide (TiO_2) as a dopant for improving power factor. Additionally, the calcination process enhances the power factor to varying degrees in all samples. The variations

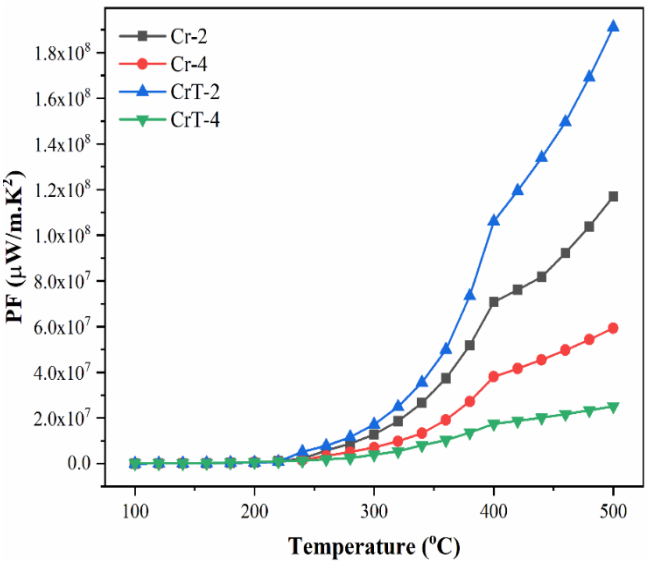

Figure 8. Power factor of different $CuCrO_2$ samples as a function of temperature.

in power factor values can be attributed to the interplay between resistivity and Seebeck coefficient [29]. In addition, the elevating the dislocation density can result in a reduction of carrier mobility within the $CuCrO_2$ system, ultimately leading to a diminished power factor [19]. While resistivity plays a role in hindering electrical conductivity, the Seebeck coefficient influences the ability of the material to generate a voltage gradient [28,30]. Optimizing this delicate balance is key to enhancing thermoelectric efficiency.

4. Conclusions

In conclusions, the addition of Ti dopants, coupled with variations in calcination processes, has been shown to impact the material's electrical properties. CrT-2, synthesized with a two-time calcination process and Ti dopant, displayed the highest power factor values, showcasing the effectiveness of titanium oxide (TiO_2) as a dopant for enhancing thermoelectric efficiency. In contrast, Cr-4, which underwent four calcination cycles, exhibited slightly lower power factor values than Cr-2. However, CrT-4, showed the lowest power factor values, potentially due to interactions between the dopant and the longer calcination process. These findings offer insights into the complexity of optimizing thermoelectric properties and highlight the potential for tailoring such materials for diverse applications in various fields, from electronics to sustainable energy technologies.

Acknowledgements

Materials and Metallurgical Characterization Laboratories Serpong, National Research and Innovation Agency Advanced Characterization Laboratories Serpong, National Research and Innovation Agency.

References

[1] S. Sharma, S. Shriwastava, S. Kumar, K. Bhatt, and C. C. Tripathi, "Alternative transparent conducting electrode materials for flexible optoelectronic devices," *Opto-Electronics Review*, vol. 26, no. 3, pp. 223-235, 2018

[2] E. Estananto, L. Utari, N. L. W. Septiani, D. Bonardo, A. Nuruddin, S. Suyatman, and B. Yuliarto, "Anatase TiO_2 on graphene-coated cotton flexible sensor at room temperature," 2023, p. 050032.

[3] R. Sitharthan, M. Ponnusamy, M. Karthikeyan, and D. S. Sundar, "Analysis on smart material suitable for autogenous micro-electronic application," *Materials Research Express*, vol. 6, no. 10, p. 105709, 2019

[4] X. Sun, Y. Wang, K. Li, J. Wang, X. Dai, D. Chong, J. Yan, and H. Wang, "Anisotropic electrical conductivity and isotropic seebeck coefficient feature induced high thermoelectric power factor > 1800 μ W m −1 K −2 in MWCNT films," *Advanced Functional Materials*, vol. 32, no. 29, p. 2203080, 2022

[5] T. N. M. Ngo, T. T. M. Palstra, and G. R. Blake, "Crystallite size dependence of thermoelectric performance of $CuCrO_2$," *RSC Advances*, vol. 6, no. 94, pp. 91171-91178, 2016

[6] F. A. Benko, and F. P. Koffyberg, "$CuCrO_2$ properties," vol. 21, no. c, pp. 753-757, 1986 .

[7] A. Liu, H. Zhu, M. Kim, J. Kim, and Y. Noh, "Engineering copper iodide (CuI) for multifunctional p-type transparent semiconductors and conductors," *Advanced Science*, vol. 8, no. 14, p. 2100546, 2021

[8] X. Chu, J. Tao, S. Li, S. Ji, and C. Ye, "Sandwich-structured silver nanowire transparent conductive films with 3H hardness and robust flexibility for potential applications in curved touch screens," *Nanomaterials*, vol. 9, no. 4, p. 557, 2019

[9] K. Ohno, T. Okada, T. Kawashima, and K. Washio, "Effect of forming gas annealing on improvement in crystal orientation of solid-phase calcined $CuCrO_2$ thin film," *Thin Solid Films*, vol. 714, p. 138386, 2020

[10] A. K. Keyan, C.-L. Yu,R. Rajakumaran,S. Sakthinathan, C. F. Wu, V. Sivaramakrishnan, S-M.Chen, and T-W. Chiu, "Highly sensitive and selective electrochemical detection of dopamine based on $CuCrO_2$-TiO_2 composite decorated screen-printed modified electrode," *Microchemical Journal*, vol. 160, p. 105694, 2021

[11] C.-C. Wang, C.-L. Yu, S. Sakthinathan, C.-Y. Chen, T.-W. Chiu, and Y.-S. Fu, "Preparation and characterization of $CuCrO_2$–CeO_2 nanofibers by electrospinning method," *Journal of Materials Science: Materials in Electronics*, vol. 33, no. 2, pp. 1091-1100, 2022

[12] H. Badr, I. S. El-Mahallawi, F. A. Elrefaie, and N. K. Allam, "Low-temperature thermoelectric performance of novel polyaniline/iron oxide composites with superior Seebeck coefficient," *Applied Physics A*, vol. 125, no. 8, p. 524, 2019

[13] Z. Bai, S.-C. Chen, S-S. Lin, Q. Shi, Y-B. Lu, S-M. Song, and H. Sun, "Review in optoelectronic properties of p-type $CuCrO_2$ transparent conductive films," *Surfaces and Interfaces*, vol. 22, p. 100824, 2021

[14] R. Manickam, J. Yesuraj, and K. Biswas, "Doped $CuCrO_2$: A possible material for supercapacitor applications," *Materials Science in Semiconductor Processing*, vol. 109, no. January, p. 104928, 2020

[15] C.-F. Wu, T.-W. Chiu, and Q. Han, "Synthesis of $CuCrO_2$-TiO_2 composite nano powder by a self-combustion glycine nitrate process," *Ceramics International*, vol. 44, pp. S76-S79, 2018

[16] H. Sun, S.-C. Chen, P.-J. Chen, S.-L. Ou, C.-Y. Liu, and Y.-Q. Xin, "p-type conductive NiOx: Cu thin films with high carrier mobility deposited by ion beam assisted deposition," *Ceramics International*, vol. 44, no. 3, pp. 3291-3296, 2018

[17] B. Szyszka, W. Dewald, S. K. Gurram, A. Pflug, C. Schulz, M, Siemers, V. Sittinger, and S. Ulrich, "Recent developments in the field of transparent conductive oxide films for spectral selective coatings, electronics and photovoltaics," *Current Applied Physics*, vol. 12, pp. S2-S11, 2012

[18] R. Manickam, and K. Biswas, "Double doping induced power factor enhancement in $CuCrO_2$ for high temperature thermoelectric application," *Journal of Alloys and Compounds*, vol. 775, pp. 1052-1056, 2019

[19] P. K. Jamshina Sanam, M. Shah, and P. P. Pradyumnan, "Structure induced modification on thermoelectric and optical properties by Mg doping in $CuCrO_2$ nanocrystals," *Solid State Communications*, vol. 353, p. 114855, 2022

[20] M. Sun, J. Shu, C. Zhao, J. Wu, H. Guo, Y. Guo, X. Yin, Y. Lin, Z. Tan, M. He, and L. Wang, "Interface Modification with $CuCrO_2$ nanocrystals for highly efficient and stable planar perovskite solar cells," *ACS Applied Materials & Interfaces*, vol. 14, no. 11, pp. 13352-13360, 2022

[21] T. Okada, S. Usui, T. Kawashima, and K. Washio, "Investigation of crystallinity, electrical conductivity, and optical transmittance of Mg-doped $CuCrO_2$ deposited on buffer layer," *Materials Science in Semiconductor Processing*, vol. 134, p. 106030, 2021

[22] H. Pan, Y. He, and X. Zhang, "Interactions between dislocations and boundaries during deformation," *Materials*, vol. 14, no. 4, p. 1012, 2021

[23] E.-H. Lee, E.-B. Kim, M. S. Akhtar, and S. Ameen, "Delafossite $CuCrO_2$ nanoparticles as possible electrode material for electro-chemical supercapacitor," *Ceramics International*, vol. 48, no. 12, pp. 16667-16676, 2022

[24] S. A. Khandy, and J.-D. Chai, "Strain engineering of electronic structure, phonon, and thermoelectric properties of p-type half-Heusler semiconductor," *Journal of Alloys and Compounds*, vol. 850, p. 156615, 2021

[25] V. Evang, J. Reindl, L. Schäfer, A. Rochotzki, P. Pletzer-Zelgert, M. Wuttig, and R. Mazzarello, "Thermally controlled charge-carrier transitions in disordered PbSbTe chalcogenides," *Advanced Materials*, vol. 34, no. 3, p. 2106868, 2022

[26] S. J. Blundell, and K. M. Blundell, *Concepts in thermal physics*. Oxford University Press on Demand, 2010.

[27] Y. Guo, X. He, W. Huang, and M. Wang, "Microstructure effects on effective gas diffusion coefficient of nanoporous materials," *Transport in Porous Media*, vol. 126, no. 2, pp. 431-453, 2019

[28] E. Karvannan, V. Vijay, T. S. Nivin, J. Archana, M. Navaneethan, and A. Karthigeyan, "Enhanced thermoelectric performance of iso-valent Al substituted Bi_2S_3 via carrier tuning and multiscale phonon scattering," *Materials Chemistry and Physics*, p. 128506, 2023

[29] M. Pandian, A. Krishnaprasanth, M. Palanisamy, G. Bangaru, R. Meena, C-. Dong, and A. Kandasami, "Effects of heavy ion irradiation on the thermoelectric properties of $In_2(Te1-xSex)_3$ Thin Films," *Nanomaterials*, vol. 12, no. 21, p. 3782, 2022

[30] P. Lin, J. Lin, S. Tung, T. Higashihara, and C. Liu, "Synergistic Interactions in sequential process doping of polymer/single-walled carbon nanotube nanocomposites for enhanced n-type thermoelectric performance," *Small*, p. 2306166, 2023.